Dynamical phase diagram of the dc-driven underdamped Frenkel-Kontorova chain

Maxim Paliy,[1,2] Oleg Braun,[2] Thierry Dauxois,[3] and Bambi Hu[1,4]
[1]*Centre for Nonlinear Studies and Department of Physics, Hong Kong Baptist University, Kowloon Tong, Hong Kong*
[2]*Institute of Physics, Ukrainian Academy of Sciences, 46 Science Avenue, UA-252022 Kiev, Ukraine*
[3]*Laboratoire de Physique, Ecole Normale Supérieure de Lyon, 46 Allée d'Italie, 69364 Lyon Cédex 07, France*
[4]*Department of Physics, University of Houston, Houston, Texas 77204*
(Received 10 April 1997)

The multistep dynamical phase transition from the locked to the running state of atoms in response to a dc external force is studied by molecular-dynamics simulations of the generalized Frenkel-Kontorova model in the underdamped limit. We show that the hierarchy of transition recently reported [Braun *et al.*, Phys. Rev. Lett. **78**, 1295 (1997)] strongly depends on the value of the friction constant. A simple phenomenological explanation for the friction dependence of the various critical forces separating intermediate regimes is given. [S1063-651X(97)08410-9]

PACS number(s): 05.70.Ln, 46.10.+z, 66.30.−h, 63.20.Ry

I. INTRODUCTION

The nonlinear response of a system of interacting atoms to a dc driving force has recently attracted great interest (see [1–10] and references therein). Knowledge of the *microscopic* mechanisms for mobility, friction, and lubrication processes is very important; in particular, for a better understanding of solid friction at the *macroscopic level*, as well as in various fields of applied science and technology such as adhesion, contact formation, friction wear, lubrication, fracture, etc.

One generic example represents a layer of atoms adsorbed on a crystalline surface. The adsorbate in this case is considered an atomic subsystem and the remainder is modeled as an external potential, a damping constant, and a thermal bath. Such a system can be treated within the framework of a generalized Frenkel-Kontorova (FK) model [11–13]. When an external dc force is applied to such a system, its response can be very nonlinear and complex. By contrast, the driven motion of a single Brownian particle in the external periodic potential has been studied in detail and is now well understood [14]. If the force F is applied to the particle, the total external potential in the direction x of the force is a corrugated plane, with a slope F. For small forces the potential has local minima, and the particle is *locked*. The local minima disappear at forces higher than $F_{f0} \equiv C\pi\varepsilon/a$, where ε is the amplitude of the periodic potential, a its period, and C a numerical factor depending on the shape of the potential. Thus, when the applied force is adiabatically increased, the atom passes from the locked to the *running* state at F_{f0}, and the mobility $B=\langle v\rangle/F$ (where $\langle v\rangle$ is the drift velocity) reaches its maximal value $B_f \equiv 1/m\eta$, where m is the atomic mass and η the friction coefficient. On the other hand, if one decreases the force F adiabatically starting from the running state, the critical force $F_{b0} \simeq 4\eta\sqrt{m\varepsilon}/\pi$ for the backward transition to the locked state is different owing to inertia of the system. Namely, in the underdamped limit ($\eta \ll \omega_0$, where ω_0 is the frequency of atomic vibration in the external potential), the inequality $F_{b0} < F_{f0}$ holds, and one can observe *hysteresis*: in the *bistable* region $F_{b0} < F < F_{f0}$, the particle is either locked or running depending on its initial velocity. For a single particle, the bistability disappears at any nonzero temperature. Besides, since the ''forward'' critical force F_{f0} is independent of the friction, and the ''backward'' force F_{b0} grows linearly with friction, the width of hysteresis vanishes at $\eta > \eta^* \equiv (C\pi^2/4a)\sqrt{\varepsilon/m}$.

The problem of *interacting* particles in a periodic potential is much more difficult. For the overdamped case ($\eta \gg \omega_0$) the nonlinear mobility of the FK model has been studied in a number of papers [1–4,9]. By contrast, investigations of the underdamped case are very limited. In that context, Persson [6] observed a *hysteretic* dynamical phase transition, similar to the $T=0$ one-particle case, in the MD simulation of a two-dimensional (2D) system of interacting atoms subjected to a periodic potential. Besides, our recent work [10] on the underdamped generalized FK model revealed strong collective effects in the dynamics of the dc-force-driven layer of atoms. When the external force increases, the FK system exhibits a complex hierarchy of first-order dynamical phase transitions from the completely immobile state to the totally running state, passing through several ''slip-stick'' intermediate stages characterized by the running state of collective *quasiparticle* excitations of the FK model known as kinks [10]. The scenario of these intermediate transitions depends on whether the concentration of atoms corresponds to trivial or complex atomic structure. All the observed transitions are hysteretic and, it is remarkable that, by contrast with the case of noninteracting atoms, the hysteresis survives at *nonzero* temperature of the system.

However, the results [10] have been obtained for one value of the friction constant η only. That is why in the present work we are interested in the question of how the observed dynamical transitions evolve when the friction changed. We calculate dynamical ''phase diagrams'' of the FK system in the (F,η) plane for two generic atomic concentrations (Sec. III). We show that several critical forces, separating intermediate stages during the transition from the locked state to the running state of the atoms are friction dependent, and we propose a simple phenomenological approach (Sec. IV) that allows one to explain these dependences.

II. MODEL

The detailed description of the generalized FK model under study, of the numerical procedure, and also the substantiation of the choice of model parameters can be found in Ref. [10]; here we only outline the main aspects of the model. The atomic motion is governed by the Langevin equation

$$m\ddot{x}_i + m\eta\dot{x}_i + \frac{d}{dx_i}\left[V_{\rm sub}(x_i,y_i,z_i) + \sum_{j(j\neq i)} V_{\rm int}(|\vec{r}_i - \vec{r}_j|)\right] = F^{(x)} + \delta F_i^{(x)}(t) \quad (1)$$

for the x coordinate of the ith atom, and similar equations for y and z. Here m is the atomic mass, $V_{\rm sub}(x,y,z)$ the external substrate potential, $V_{\rm int}(r)$ the potential of pairwise interaction between atoms, η the viscous friction constant, which corresponds to the rate of energy exchange with the substrate, $\vec{F}=\{F,0,0\}$ the dc driving force, and $\delta\vec{F}$ the Gaussian random force with correlation function

$$\langle \delta F_i^{(\alpha)}(t)\,\delta F_j^{(\beta)}(t')\rangle = 2\eta m k_B T \delta_{\alpha\beta}\delta_{ij}\delta(t-t'). \quad (2)$$

For a better representation of the natural microscopic scale of the problem, we use a dimensional system of units, measuring distance in angstrom, energy and temperature in electronvolts. The mass of atoms is chosen as unity: $m=1$. In the remainder of the paper, the units of other dimensional physical quantities are omitted, but they are expressed in terms of the above units.

We use exponential interactions between atoms corresponding to the repulsion between atomic cores,

$$V_{\rm int}(r) = V_0 \exp(-\beta_0 r), \quad (3)$$

where $V_0=10$ eV is the amplitude and inverse of $\beta_0=0.85$ Å^{-1} determines the range of interaction.

To model the substrate, we used in the simulation the true 3D external potential, periodic in the (x,y) plane (with the rectangular symmetry) and parabolic in the z direction,

$$V_{\rm sub}(x,y,z) = V_{\rm pr}(x;a_{sx},\varepsilon_{sx},s_x) + V_{\rm pr}(y;a_{sy},\varepsilon_{sy},s_y) + \tfrac{1}{2}m\omega_z^2 z^2, \quad (4)$$

where ω_z is the frequency of normal vibration of a single atom, and

$$V_{\rm pr}(x;a,\varepsilon,s) = \frac{1}{2}\varepsilon\frac{(1+s)^2[1-\cos(2\pi x/a)]}{1+s^2-2s\cos(2\pi x/a)} \quad (5)$$

is the deformable Peyrard-Remoissenet potential [15], and the parameter s, $|s|<1$, describes its shape. The choice of the lattice constants, $a_{sx}=2.74$ Å, and $a_{sy}=4.47$ Å, and of the energy barriers, $\varepsilon_{sx}=0.46$ eV and $\varepsilon_{sy}=0.76$ eV, provide a high anisotropy of this potential, which can be viewed as the set of ''channels'' with corrugated bottoms, oriented along the x direction. This potential is typical for the furrowed crystal surfaces, namely, our parameters were chosen for the Na-W(112) adsystem [10]. The frequency ω_x of a single-atom vibration along the x direction is connected to the shape parameter s_x by the relationship $\omega_x=\omega_0(1+s_x)/(1-s_x)$, where $\omega_0\equiv(\varepsilon_{sx}/2m)^{1/2}(2\pi/a_{sx})$. We have chosen typical values $s_x=0.2$ and $s_y=0.4$, which lead to the frequencies of atomic vibrations $\omega_x=1.65$ and $\omega_y=2.02$, respectively. Finally, we took $\omega_z=\frac{1}{2}(\omega_x+\omega_y)=1.84$. Note that our choice of parameters does not claim to be a quantitative interpretation of the concrete adsystem, because the model is oversimplified. However, we do believe in a qualitative description of the effect under investigation and claim that typical adsystems should exhibit similar behaviors.

In the present work we study the behavior of the system in a wide range of frictions in the underdamped limit $\eta \ll \omega_x$, corresponding to typical adsystems [16]. In the simulation, we first look for the minimum-energy configuration of the system. Then, we adiabatically increase temperature and force and measure the mobility B for given values T and F (this procedure was described in detail in [10]). In order to emphasize the phase transitions, the system is studied at a very low substrate temperature, $T=0.0005$ eV.

An important parameter of the generalized FK model is the atomic concentration. For the repulsive interatomic interaction used in the present work, we have to impose the periodic boundary conditions in the x and y directions in order to fix the concentration. Namely, we place N atoms into the fixed area $L_x\times L_y$, where $L_x=M_x a_{sx}$ and $L_y=M_y a_{sy}$, so that the dimensionless atomic concentration (the so-called coverage in surface physics) is equal to $\theta=N/M$ $(M=M_xM_y)$. The atomic concentration in the FK system plays a crucial role since it defines the number of quasiparticle excitations, i.e., the number of geometrical (residual) kinks. These excitations can be defined for any background *commensurate* atomic structure $\theta_0=p/q$, where p and q are relative prime integers [13,17]. If the concentration θ slightly deviates from the background value θ_0, the ground state of the system corresponds to large domains with background commensurate coverage θ_0, separated by localized incommensurate zones of compression (expansion) called kinks (antikinks). When the background commensurate coverage is *trivial*, $\theta_0=1/q$, the kinks defined on this structure are called *trivial* kinks [13]. Besides, a nontrivial background coverage $\theta_0=p/q$ $(p\neq 1$, with complex elementary cells consisting of p atoms) can be represented as a lattice of trivial kinks, defined on the background of the closest trivial structure. Therefore, in the latter case a deviation from the $\theta_0=p/q$ structure can be represented as a discommensuration in the lattice of trivial kinks, i.e., a ''kink in the kink lattice,'' called *superkink* [13].

As in the simulation we study finite systems, we have to choose an appropriate system size to insert N_k kinks into the $\theta_0=p/q$ commensurate background structure; the integers N and M must satisfy the equation [17]

$$qN = pM + N_k\sigma, \quad (6)$$

where the topological charge σ is $\sigma=+1$ for the kink and $\sigma=-1$ for the antikink. As background structures, we discuss here two interesting cases, the trivial coverage $\theta_0=1/2$, and the complex coverage $\theta_0=2/3$.

III. SIMULATION RESULTS

To simplify the problem, in the present work we only consider the quasi-one-dimensional case, putting $M_y=1$, so that all chains move in the same way (however, the interaction between the atoms, as well as the atomic motion, still has 3D character). Let us note here that this simplified choice leads only to a minor difference in system behavior in comparison with true 2D FK system with $M_y>1$ [10]. Namely, the exact critical force depends slightly on the external conditions, which means that the transitions do not occur simultaneously in all the chains. A careful examination of the behavior in different chains shows an enhanced transition to sliding state due to cooperative effects in the second dimension with an exponential law [10]. On the contrary, the transition of a chain to the locked state is almost independent of neighboring chains.

A. Trivial $\theta_0=1/2$ background coverage

First, let us consider the ground state, which corresponds to domains of the trivial $\theta_0=1/2$ coverage separated by trivial kinks: $\theta=21/40$. Namely, we took $N=105$ and $M_x=200$, having thus ten kinks over the length under investigation with an average spacing of $20a_{sx}$ between kinks.

The generic $B(F)$ dependence for the friction constant $\eta=0.12\omega_x$ is presented in Fig. 1(a). In this figure, as well as in all figures below, it will be convenient to express force F in units of the constant ''forward'' critical force for a single particle $F_{f0}=C\pi\varepsilon_{sx}/a_{sx}\approx 0.607$ ($C\approx 1.15$ for the shape of the external potential used in the present simulation). During the force-increasing process, one can distinguish several steps in the $B(F)$ dependence, which correspond to a hierarchy of depinnings of kinks [10]. Namely, at $F<F_{tk}\approx 0.23F_{f0}$ the system is in the completely immobile state, while at $F>F_{tk}$ the system has nonzero mobility B_{tk} due to the *running state* of trivial kinks [Fig. 2(a)]. It was shown in [10] that the force F_{tk} is related to the degradation of the periodic Peierls-Nabarro potential $\varepsilon_{\rm PN}$ for the trivial kinks: the kinks start to slide at $F>F_{tk}\approx\pi\varepsilon_{\rm PN}/a_{ax}$. The second abrupt increase of the mobility to the value B_m takes place when the force exceeds a certain threshold $F_{\rm pair}\approx 0.35F_{f0}$, connected with the vanishing of the energy barrier for creation of additional kink-antikink pairs in the system, so the number of mass carriers in the system increases, leading to the increase of the mobility. The remarkable tendency for the running kinks is to come closer to each other, thus bunching into compact groups. This tendency is especially enhanced after the second threshold $F_{\rm pair}$, where the concentration of kinks is large. The bunched kinks build up dense groups of immobile atoms with $\theta=1$, while the rest of the system consists of running atoms (corresponding to the running state of force-excited antikinks). This state, which is very reminiscent of a *traffic jam* [Fig. 2(b)], survives until the last threshold force $F_f\approx 0.53F_{f0}$, after which all the atoms are sliding over the periodic potential, and the system reaches the highest possible value of the mobility $B_f=1/m\eta$.

During the force-decreasing process, the system jumps back to the immobile state at the critical force F_b, and one can see a large hysteresis, which, contrary to the one-particle case, survives at nonzero temperature [10].

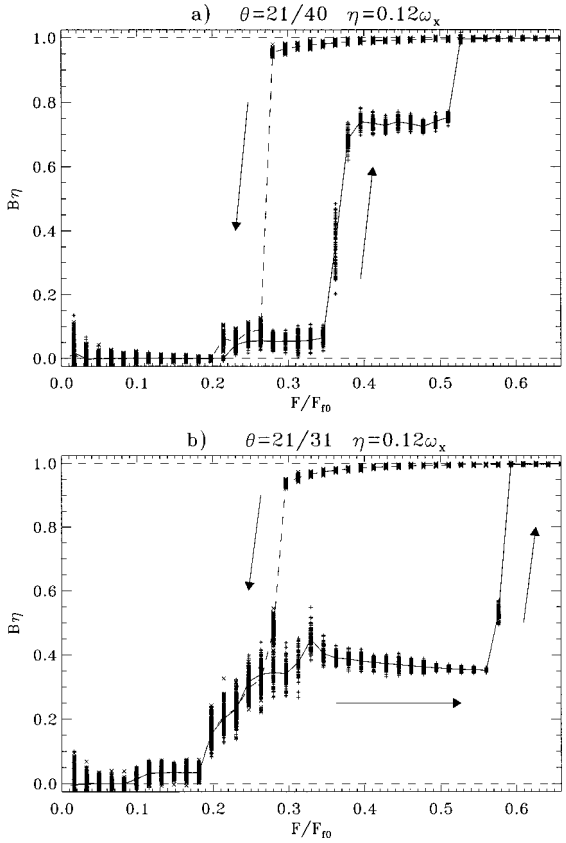

FIG. 1. The mobility B vs external force F for the quasi-one-dimensional FK model: (a) for $\theta=21/40$ coverage (trivial kinks on the background of trivial $\theta_0=1/2$ structure); (b) for $\theta=21/31$ coverage (superkinks on the background of the complex $\theta_0=2/3$ structure). The plus signs and the solid curve correspond to increasing force, the cross signs and the dashed curve to decreasing force. The arrows indicate the hysteresis. The force F is expressed in terms of the ''forward'' force for a single atom $F_{f0}=C\pi\varepsilon_{sx}/a_{sx}$ defined in the Introduction.

As mentioned in the Introduction, for a single Brownian particle the ''forward'' force F_{f0} is independent of the friction, while the ''backward'' force F_{b0} is linearly proportional to the friction. By contrast, the situation is more complex in the case of interacting atoms. Figure 3 represents the dynamical phase diagram in the (F,η) plane, where we plot the critical forces F_{tk}, $F_{\rm pair}$, F_f, and F_b versus the friction coefficient η.

Let us consider first the forward transition from the locked to the running state. One can distinguish two regions of friction corresponding to different scenarios of the transition.

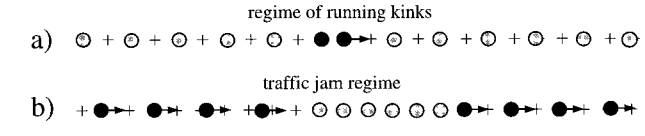

FIG. 2. Illustration of the atomic motion in the regime of running kinks (a) and in the ''traffic jam'' regime (b). Immobile atoms are denoted by gray circles, running atoms and atoms in the kink regions are denoted by black circles; arrows indicate the direction of atomic motion.

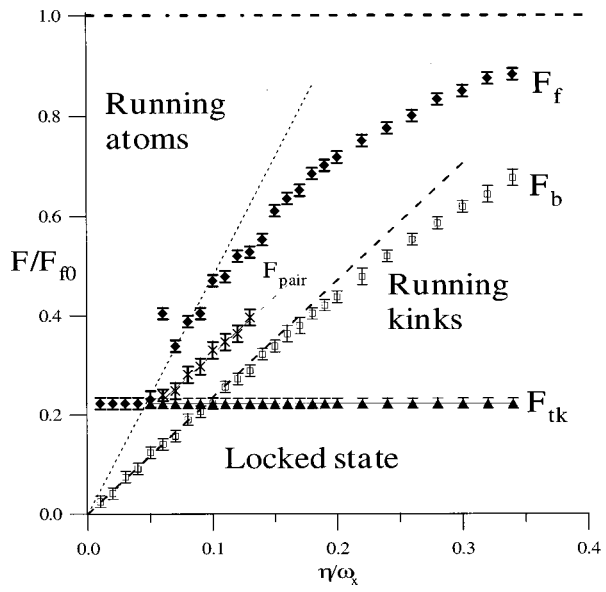

FIG. 3. Dynamical phase diagram in the (F,η) plane for the quasi-one-dimensional FK model at the $\theta=21/40$, i.e., for the trivial kinks on the background of simple $\theta_0=1/2$ structure. The force F is scaled in the same way as in Fig. 1.

(i) At very low frictions, $\eta<0.05\omega_x$, there are no intermediate stages. When the force increases, the system jumps from the locked to the running state directly at the force F_f, this force being exactly equal to the critical force F_{tk} for the *kink* transition to the running state.

(ii) By contrast, at larger frictions, $\eta>0.05\omega_x$, all the above-mentioned intermediate stages with running kinks do exist. The second difference from the very low friction region is that the ''forward'' force F_f and the kink-antikink nucleation force $F_{\rm pair}$ are *friction-dependent*, namely, they grow with friction increasing, while the critical ''kink'' force F_{tk} remains constant. At not too high frictions, the critical force F_f first increases approximately linearly with the friction η, while at higher frictions the increase of F_f slows down, and finally tends to a constant value F_f^*, close to the value F_{f0} for noninteracting atoms (Fig. 3).

Unfortunately, we failed to plot the critical force $F_{\rm pair}$ in Fig. 3 at $\eta>0.14\omega_x$, because the ''traffic jam'' regime is not well defined anymore at these higher frictions, probably because of the small number of atoms in the immobile group [Fig. 2(b)] at $\theta=21/40$ for the finite-size system. However, at a higher concentration $\theta=21/31$ (see next subsection III B), where the immobile groups are larger, the ''traffic jam'' regime is well defined at all studied frictions.

The backward transition from the running to the locked state has one interesting feature. Namely, the ''backward'' critical force F_b grows with η increasing [notice that at not too high frictions, $F_b(\eta)$ exactly matches the law $F_{b0}\simeq 4\eta\sqrt{m\varepsilon_s}/\pi$ for *noninteracting* atoms, shown by the dashed line in Fig. 3]. If the friction is high enough, F_b is larger than the critical force for kinks $F_{tk}=$const. Therefore, at $\eta<0.1\omega_x$ the system jumps back to the completely *locked* state of atoms, while at $\eta>0.1\omega_x$ the backward transition has also a multistep character: when the force decreases, first a drop of the mobility B from B_f to kink-mobility value B_{tk} occurs, and only at some $F<F_{tk}$ the mobility vanishes finally.

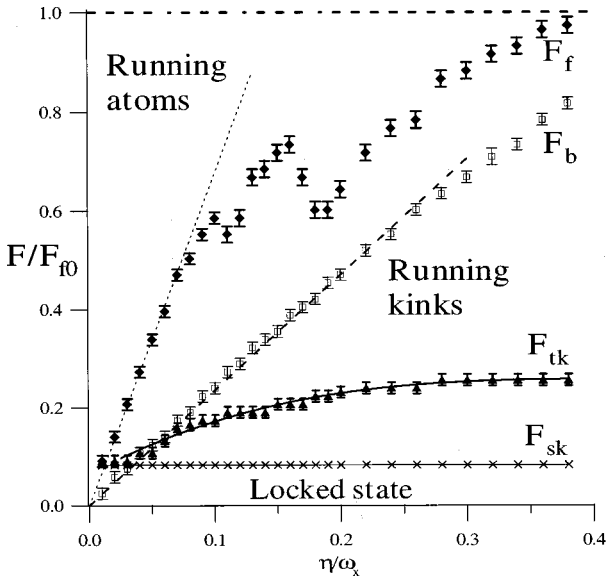

FIG. 4. Dynamical phase diagram in the (F,η) plane for the $\theta=21/31$ coverage. The force F is scaled in the same way as in Fig. 1.

B. Complex $\theta_0=2/3$ background coverage

Now let us describe the behavior of the system at the concentration $\theta=21/31$ (we used $N=105$ and $M_x=155$). The ground state in this case corresponds to domains of complex $\theta_0=2/3$ commensurate structure, separated by *superkinks* with an average spacing $30a_{sx}$ between them. On the other hand, the $\theta=2/3$ structure can be viewed as a dense lattice of *trivial* kinks defined on the background of the $\theta_0=1/2$ structure.

This specificity clearly manifests itself in the $B(F)$ dependence plotted in Fig. 1(b) for the same friction constant $\eta=0.12\omega_x$ as in Fig. 1(a). During the force-increasing process, one can distinguish two sharp steps of increasing of the mobility B. The first one, at $F\approx F_{sk}=0.08F_{f0}$, corresponds to the situation where the *superkinks* start to slide [10], whereas the second step, occurring at $F\approx 0.18F_{f0}$ for $\eta=0.12\omega_x$, corresponds to the transition of the *trivial* kinks to the running state, as can be seen from the phase diagram in Fig. 4. At higher forces the increase of the mobility is smoother, and the system again reaches an intermediate *traffic jam* regime with $B=B_m$, where the mobility depends on the coverage as $B_m(\theta)\propto B_f(1-\theta)/\theta$, $B_f=1/m\eta$ being the maximum mobility [10].

The dynamical phase diagram (F,η) for the complex coverage $\theta=21/31$ is shown in Fig. 4, where we plot F_{tk}, F_f, F_b (as in Fig. 3) and, additionally, F_{sk}. However, $F_{\rm pair}$ is not plotted because the system goes to the ''traffic jam'' regime quite smoothly, and therefore it is difficult to resolve $F_{\rm pair}$.

One can see first that the critical force for superkinks F_{sk} is independent of friction, while the force F_{tk} increases with the friction η and reaches the constant value $F_{tk}\approx 0.24F_{f0}$ at high friction, which almost exactly matches the value $F_{tk}\approx 0.23F_{f0}$ for the case of $\theta=21/40$ coverage.

The noticeable difference with the case of $\theta=21/40$ coverage is in the dependence of the forward critical force $F_f(\eta)$. *First*, as the value of F_{sk} is very low, the low-friction region with $F_f=\text{const}$ is very narrow ($\eta<0.01\omega_x$), and was not resolved in the simulation. *Second*, the initial linear increase of F_f with η has a larger slope than for the $\theta=21/40$ case; at high frictions the critical force F_f also tends to a constant value $F_f^*\approx F_{f0}$. *Third*, there are some irregularities in the $F_f(\eta)$ dependence at intermediate frictions. Namely, from the plots $B(F)$ at higher frictions [similar to the case plotted in Fig. 1(b)] we found that in the ''traffic jam'' regime the mobility does not have a constant value B_m as for lower frictions [the last plateau in Fig. 1(b)], but at certain intervals of frictions $B(F)$ exhibits an additional plateau with a larger value of the mobility, $B=B_m'$ ($B_m<B_m'<B_f$). This should result in a lower value of the critical force F_f due to the larger kinetic energy of the system in this intermediate state (see discussion in the next section).

Finally, we observed that the ''backward'' critical force F_b is almost independent of coverage, and its dependence on friction is again well described by the corresponding expression for noninteracting atoms.

IV. DISCUSSION

The most interesting feature of both phase diagrams in Figs. 3 and 4 is that the critical forces, separating various intermediate stages during the forward transition, are *friction dependent*, except the first critical force, which corresponds to the completely locked *preceding* stage. From this, we may conclude that the kinetic energy of the system in the *preceding* stage defines the transition to the *following* stage. Below we present a discussion that allows one to rationalize the contribution of the kinetic energy of the running kinks to the dynamical phase transition towards the running state of atoms.

First let us consider the lowest interval of frictions, $\eta<0.1\omega_x$ in the phase diagrams of Figs. 3 and 4. The explanation of the dependence of F_f on friction η in this region can be done solely with the help of kinetic arguments in the following way. Assume that there is a ''critical'' velocity of kink v_c, above which the *running* kink cannot exist as a stable quasiparticle (as was found by Peyrard and Kruskal [18], such a critical velocity does exist for the running kinks in the frictionless case). Then, if at given values of the force F and the friction η the kink drift velocity $\langle v_k\rangle=F/m_k\eta_k$ is higher than v_c, the kink should destroy itself as soon as it starts to move, this immediately will cause an avalanche driving the whole system to the totally running state of atoms.

If one makes the simplifying assumption that $\eta_k\sim\eta$, the drift velocity of kinks is $\langle v_k\rangle\propto F/\eta$ and, therefore, the region in the phase diagram (F,η), where the running kinks are stable, is bounded by the straight line $F\propto v_c\eta$. This simple linear dependence describes quite well the dependence $F_f(\eta)$ for $\eta<0.1\omega_x$ (see dotted lines in Figs. 3 and 4). Thus, for instance, in the $\theta=21/40$ case (Fig. 3) for $\eta<0.05\omega_x$, when the applied force exceeds the threshold F_{tk}, the stationary drift velocity for the kink is higher than v_c, and the system goes directly to the running state of atoms. This mechanism provides that $F_f=F_{tk}=$ const in this region. However, at higher frictions, $\eta>0.05\omega_x$, the kink can move as a stable quasiparticle, and the transition to the running state takes place at a higher force $F_f\propto\eta$ (Fig. 3). Such a linear dependence holds also (and even better) for the coverage $\theta=21/31$ at not too high friction (see Fig. 4). Unfortunately, we failed to find the value of the critical velocity explicitly, because we do not know the values for the kink mass m_k and the friction coefficient η_k. However, we observed that this critical velocity v_c is proportional to the sound velocity c [defined as $c^2\approx a_A^2V_{\text{int}}''(a_A)$, where $a_A=a_{sx}/\theta_0$ is the average interatomic distance along the chain]. Indeed, from the slopes of dotted lines in Figs. 3 and 4 the ratio of the critical velocities for both studied coverages is $v_c^{(21/40)}/v_c^{(21/31)}\approx 0.72\pm 0.07$, and the corresponding ratio of the sound velocities for the background coverages is $c^{(1/2)}/c^{(2/3)}=0.74$.

At higher frictions, $\eta>0.1\omega_x$, F_f starts to deviate significantly from the simple linear law, and finally tends to a constant value F_f^*. This behavior may be qualitatively explained if we take into account that the *running* kinks stimulate the transition of the system to the totally running state. Indeed, owing to their nonzero kinetic energy T_{kink}, the running kinks effectively reduce the average energy barrier for the transition of all the atoms to the running state; therefore the effective barrier ε_{eff} should be lower than ε_{sx}. Let us approximate the effective barrier as $\varepsilon_{\text{eff}}=\varepsilon_{sx}-T_{\text{kink}}$, where $T_{\text{kink}}\propto\langle v_k\rangle^2\propto F^2/\eta^2$. Then, the critical force for the transition to the running state, $F_f=C\pi\varepsilon_{\text{eff}}/a_{sx}$, is determined by the following equation:

$$\frac{\alpha}{\eta^2}F_f^2+F_f=F_f^*, \tag{7}$$

where $\alpha>0$ is a phenomenological coefficient, and $F_f^*\approx F_{f0}\equiv C\pi\varepsilon_{sx}/a_{sx}$. Equation (7) provides a qualitative agreement with the simulation data: at small η the forward force is proportional to η, $F_f(\eta)=\sqrt{F_f^*/\alpha}\,\eta$, while at $\eta\to\infty$ we have $F_f\to F_f^*$. Unfortunately, the quantitative agreement is not satisfactory. Even if Eq. (7) can provide a rather good fitting of the $F_f(\eta)$ dependence in Fig. 3, the nonmonotonic peculiarities of $F_f(\eta)$ in Fig. 4 remain unexplained. We recall, however, that the main simplification made above is that the friction coefficient for the running kinks η_k is equal to η. But the running kink experiences also the *intrinsic* friction η_{int}, so that the correct expression is $\eta_k=\eta+\eta_{\text{int}}$, where η_{int} depends very nonlinearly and *resonantly* on the kink velocity $\langle v_k\rangle$ [18–20]. The intrinsic part of friction arises because the propagating kink excites small-amplitude waves (phonons) in the discrete atomic chain. At certain drift velocities the translational motion of kink (i.e., the frequency with which kinks ''hit'' the particles) can come in a resonance with the allowed phonon frequencies, which results in bigger losses of energy by kink and increases effective damping. This is very likely why one can observe nonmonotonic variation of $F_f(\eta)$ in Fig. 4.

The proposed qualitative picture may be applied not only to F_f, but also to other intermediate critical forces, such as F_{pair} or F_{tk} in the case of the complex background $\theta=21/31$ coverage. For example, the critical force for the trivial kinks F_{tk} increases with the friction in the $\theta=21/31$ case, when the

preceding stage is characterized by the running superkinks (Fig. 4); F_{tk} tends to the constant value found for trivial background coverage $\theta=21/40$ only at high frictions, when the kinetic energy contribution of superkinks to the initialization of the trivial kinks motion becomes unessential.

Finally, let us comment on the fact that the asymptotic ($\eta\to\infty$) forward critical force F_f^*, for both studied coverages, has been found to be equal to the critical force for a single atom $F_{f0}=C\pi\varepsilon_{sx}/a_{sx}$. This is easy to understand if one takes into account that the studied atomic chain corresponds to a low-coupling limit [13], because the dimensionless elastic constant $g_{\rm eff}=(a_{sx}^2/2\pi^2\varepsilon_{sx})V''_{\rm int}(a_A)$ is well below unity for both studied coverages, namely, $g_{\rm eff}\in[0.06,0.2]$ for $\theta\in[1/2,2/3]$. Therefore, the interaction between atoms should not lead to a significant change of the barrier for the transfer of an atom to the running state *unless the running kinks contribute to this transition.*

V. CONCLUSIONS

Thus, we have studied the dynamical phase transition from the locked to the running state of interacting atoms in a periodic external potential under the action of a dc external force in the underdamped limit of a generalized Frenkel-Kontorova model. This transition proceeds by a complex multistep scenario, which can be treated as a hierarchy of depinnings of quasiparticle excitations of the FK model (kinks). The interesting feature of the transition is that the critical forces separating different intermediate stages during the ''forward'' transition are friction dependent, except the first critical force, which corresponds to the transition from the completely locked ground state. This reflects the dynamical nature of transitions between intermediate stages, namely, that the kinetic energy of running kinks in the *preceding* stage significantly contributes to the transition towards the *following* stage.

On the basis of simulation results, we have proposed a phenomenological approach that qualitatively explains the observed friction dependences of the critical forces. According to this approach, for low frictions the critical quantity determining the criterion for the transition to the totally running state of atoms is the drift velocity of kinks at the preceding stage. This approach leads to the simple phenomenological equation (7) for the dependence of the forward critical force on friction. However, for a better quantitative description of the simulation results one has to take into account the resonant interaction of the running kinks with the phonons excited in the atomic chain [18–20]. Work along these lines is in progress.

ACKNOWLEDGMENTS

The authors thank Michel Peyrard for very helpful comments. All members of the Center for Nonlinear Studies at HKBU are acknowledged for stimulating discussions. The work of M.P. and B.H. was supported in part by the Research Grant Council, and the Hong Kong Baptist University Faculty Research Grants.

[1] S. E. Trullinger, M. D. Miller, R. A. Guyer, A. R. Bishop, F. Palmer, and J. A. Krumhansl, Phys. Rev. Lett. **40**, 206 (1978); **40**, 1603 (1978).
[2] R. A. Guyer and M. D. Miller, Phys. Rev. A **17**, 1774 (1978).
[3] M. Büttiker and R. Landauer, Phys. Rev. A **23**, 1397 (1981).
[4] F. Marchesoni, Phys. Rev. B **34**, 6536 (1986); P. Hänggi, F. Marchesoni, and P. Sodano, Phys. Rev. Lett. **60**, 2563 (1988); F. Marchesoni, *ibid.* **73**, 2394 (1994).
[5] J. C. Ariyasu and A. R. Bishop, Phys. Rev. B **35**, 3207 (1987).
[6] B. N. J. Persson, Phys. Rev. Lett. **71**, 1212 (1993); Phys. Rev. B **48**, 18 140 (1993).
[7] F.-J. Elmer, Phys. Rev. E **50**, 4470 (1994).
[8] Y. Braiman, F. Family, and H. G. E. Hantschel, Phys. Rev. E **53**, R3005 (1996).
[9] L. M. Floria and J. J. Mazo, Adv. Phys. **45**, 505 (1996).
[10] O. M. Braun, T. Dauxois, M. V. Paliy, and M. Peyrard, Phys. Rev. Lett. **78**, 1295 (1997); Phys. Rev. E **55**, 3598 (1997).
[11] Ya. Frenkel and T. Kontorova, Phys. Z. Sowjetunion **13**, 1 (1938).
[12] I. F. Lyuksyutov, A. G. Naumovets, and V. L. Pokrovsky, *Two-Dimensional Crystals* (Naukova Dumka, Kiev, 1983; Academic Press, Boston, 1992).
[13] O. M. Braun and Yu. S. Kivshar, Phys. Rev. B **50**, 13 388 (1994).
[14] H. Risken, *The Fokker-Planck Equation* (Springer, Berlin, 1984), and references therein.
[15] M. Peyrard and M. Remoissenet, Phys. Rev. B **26**, 2886 (1982).
[16] O. M. Braun, A. I. Volokitin, and V. P. Zhdanov, Usp Fiz. Nauk **158**, 421 (1989) [Sov. Phys. Usp. **32**, 605 (1989)].
[17] O. M. Braun, Yu. S. Kivshar, and I. I. Zelenskaya, Phys. Rev. B **41**, 7118 (1990).
[18] M. Peyrard and M. D. Kruskal, Physica D **14**, 88 (1984).
[19] O. M. Braun and Yu. S. Kivshar (unpublished).
[20] S. Watanabe, H. S. J. van der Zant, S. H. Strogatz, and T. P. Orlando, Physica D **97**, 429 (1996).